Active and Passive Elec. Comp., 1985, Vol. 12, pp. 9–32
0882-7516/85/1201-0009 $18.50/0

THIN METAL FILM SENSORS

C.R. TELLIER
Laboratoire de Chronométrie, Electronique et Piézoélectricité –
Ecole Nationale Supérieure de Mécanique et des Microtechniques, La Bouloie, 25030 BESANCON CEDEX, FRANCE

(Received April 20, 1984; in final form September 18, 1984)

During the last decade some progress have been made in the field of sensors using thin film techniques. In particular thin metal film strain gauges and thin film temperature sensors based on the temperature dependent resistivity of metal are now commonly used. But changes in other transport parameters with various measurands are also useful for the design of metal film sensors. Difficulty arises in thin film techniques when structural defects are frozen in films.

Intensive theoretical investigations are carried out to explain the effect of grain-boundary and external surface scatterings on transport parameters. Accordingly the main results are presented to specify the influence of film structure on the sensor performance. The grain-boundary effects are discussed according to applications of metal film sensors. Theoretical predictions are analyzed in terms of sensitivity, thermal stability and long term behavior. But other problems induced by the presence of grain boundaries or point defects are also discussed, in particular problems associated with bulk diffusion, electromigration induced failures or intrinsic stresses.

1. INTRODUCTION

Thin metal films can be used as thin film sensors in a number of different ways. If the thermal expansion mismatch between the film and its substrate is low enough to ensure negligible thermal strains, a thin metal film formed on the surface of a strainable substrate can constitute a strain gauge.[1–3] In the field of magnetic measurements thin metal film devices based on the transverse Hall effect can also be useful as magnetic sensors,[4] moreover applications of Hall elements are widely concerned with position sensors, contactless current sensors and so on.[5,6,7] Among all the various type of sensors that can be used to measure temperature those based on the thermoelectric effect are probably the most attractive,[5] thin metal film thermocouples provide effectively many possibilities[5,8] for temperature sensors. Moreover some of the common approaches to gas detection include the electrical conductance of thin metal films,[9] provided that the effect of film thickness is effectively marked, gas absorption at the film surface can modify significantly the film conductance.[10,11,12]

However the electric properties of thin continous metal films are very sensitive to the structure of films.[13,14] It should be pointed out that the structure of thin films depends on preparation methods and deposition conditions such as nature and temperature of the substrate surface, temperature of the evaporation or sputtering source.[15] As a result films can exhibit point defects such as vacancies and interstitials, lines of imperfections such as dislocations and surfaces of imperfections such as grain-boundaries. In most practical cases metal films have a grained structure[15–23] and it is well known that in particular, grain boundaries play decise roles in electrical properties of thin films. Thus, in the past few years some theoretical works[14,24–26] have been carried out to analyze the effect of electronic scattering at grain boundaries on the transport properties of films. Therefore this paper begins with a review of the existing theories in order to show how the grain structure and the film geometry dominate the electrical conductivity, the thermoelectric effect, the Hall effect and the electromechanical properties and thus influence the sensitivity of thin metal film sensors. The paper ends with a

discussion of the possible applications of thin metal films as sensors. Special emphasis is placed on stability of thin film sensors.

2. PHYSICAL AND MATHEMATICAL MODELS FOR TRANSPORT PROPERTIES

The physical model is based on a simplified Boltzmann equation[24-26] where a resultant relaxation time, τ^*, describes the three electronic scattering processes operating simultaneously namely isotropic background scattering due to phonons, grain-boundary scattering and external surface scattering. At this point grained films are conveniently separated with three groups (Figure 1)

i) polycrystalline films with very small average crystalline sizes, D_x, D_y and D_z measured respectively in the x-, y- and z- direction which remain always smaller than the film thickness, t.

ii) columnar films with grains extended in the vertical direction and average grain sizes D_x and D_y smaller than t.

iii) monocrystalline films exhibit average grain sizes D_x and D_y which are exactly equal to or greater than the film thickness.

According to these definitions the transport properties of grained films can be conveniently analyzed in terms of three or bi-dimensional representations of grain-boundaries (Figure 1). These are the well documented multi-dimensional models of grain boundaries discussed in several papers.[14,24-26] Thus a detailed description of these models is beyond the scope of this paper but we present the most relevant scattering parameters which can effect the sensor sensitivity. These are the surface parameter

$$\kappa = t\left[\lambda_0 \ln \frac{1}{p}\right]^{-1} \tag{1}$$

where λ_0 is the background mean free path and p is the usual specular reflexion coefficient at the external surfaces[27] and the grain parameter

$$\nu_i = D_i(\lambda_0 \ln 1/\mathscr{E})^{-1} \quad i = x, y, z \tag{2}$$

which involves the transmission coefficient $\mathscr{E}$ through the grain boundaries distributed perpendicular to the direction i.

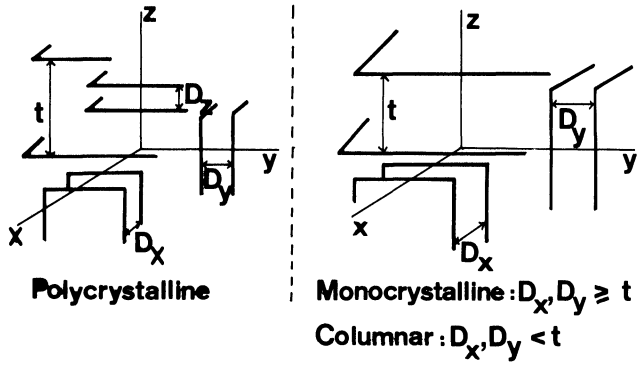

FIGURE 1 The geometry of the multi-dimensional models.

2.1. The Electrical Conductivity

In general the structure of fine grained films such as polycrystalline films can be identified with cubic like structure. For a sake of simplicity we also assume that in columnar and monocrystalline films the grain boundaries consist of two arrays with the same average spacing D. The electrical conductivity of grained film is then given by the general relation:

$$\frac{\sigma_{fj}}{\sigma_0} = \frac{3}{2} \cdot \frac{1}{b_j} f(a_j) = F(\lambda_0, t, D, \mathscr{C}, p), \quad j = c, m, p \tag{3}$$

with

$$f(a_j) = a_j - \frac{1}{2} + (1 - a_j^2) \ln (1 + a_j^{-1}), \; j = c, m, p \tag{4}$$

where σ_0 is the background conductivity. The subscript c, m, p refers respectively to columnar, monocrystalline and polycrystalline films.

The effect of grain structure is included in a_j and b_j coefficients since for columnar and monocrystalline films

$$a_{c,m} = (1 + C^2 \nu^{-1}) b_{c,m}^{-1} \tag{5}$$

with

$$C = 4/\pi \tag{6}$$

and

$$b_{c,m} = \kappa^{-1} - C \nu^{-1} \tag{7}$$

whereas for polycrystalline films

$$a_p = (1 + C^2 \nu^{-1}) b_p^{-1} \tag{8}$$

with

$$b_p = \kappa^{-1} + (1 - C) \nu^{-1} \tag{9}$$

The behavior of monocrystalline films with grain size, D, equal to film thickness, t, is illustrated in Figure 2, the conductivity ratio σ_{fm}/σ_0 is found to exhibit more pronounced size effect than the conductivity ratio of films free of grain boundaries. In contrast as shown in the inset of Figure 2 the conductivity of columnar and polycrystalline films is drastically reduced by grain-boundary scattering effect and tends in the limit of very large thickness to a limiting value which depends on the nature of scattering at grain-boundaries i.e. on the parameter ν.

The temperature, T, dependence of the electrical conductivity is an important factor for the thermal stability of thin film sensors. Thus it may be of interest to report the theoretical expression of the temperature coefficient of resistivity (t.c.r.)

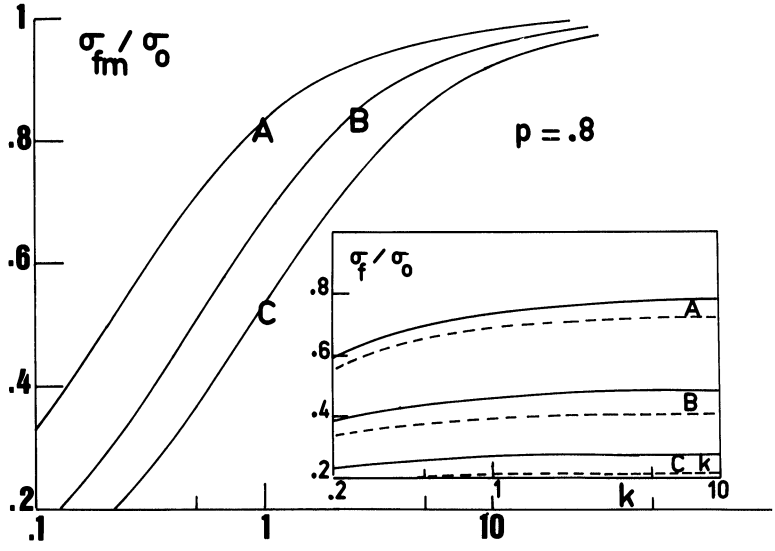

FIGURE 2 The reduced thickness dependence of the reduced monocrystalline film conductivity for p = 0.8. Curve A: $\kappa = 0.9$, Curve B: $\kappa = 7$, Curve C: $\kappa = 0.5$. The dependence of the reduced conductivity on the reduced thickness for polycrystalline films (dotted lines) and for columnar films (full lines) can be shown in the inset. Curve A: $\nu = 4$, Curve B $\nu = 1$, Curve C: $\nu = 0.4$.

for grained films which is defined as[14]

$$\beta_{fj} = d\ln \rho_{fj}/d\,T \quad j = c, m, p \tag{10}$$

If we neglect the thermal expansion mismatch between the film and its substrate and if we assume that the thermal expansion of the grain and the film thickness are negligible, with respect to that of the background mean free path the analysis leads to the general relation[14,25,28]

$$\frac{\beta_{fj}}{\beta_0} = 1 + \frac{\lambda_0}{F(\lambda_0)}\,\frac{dF(\lambda_0)}{d\lambda_0} = \frac{1}{b_j}\,\frac{g(a_j)}{f(a_j)}, \quad j = c, m, p \tag{11}$$

with

$$g(a_j) = a_j^{-1} - 2 + 2a_j \ln(1 + a_j^{-1}), \quad j = c, m, p \tag{12}$$

where

$$\beta_0 = d\ln \rho_0/dT = -\,d\ln \lambda_0/dT \tag{13}$$

is the background t.c.r.

Numerical evaluation of the product resistivity x t.c.r., $\beta_{fj}\,\rho_{fj}/\beta_0\rho_0$, reveals a very interesting feature since the relation[14]

$$\beta_{fj}\,\rho_{fj} \tilde{\sim} \beta_0\,\rho_0 \tag{14}$$

is found to be satisfied in large κ and ν ranges. Thus as the grain-boundary effects are essentially temperature independent the Matthiessen's rule[29] apparently applies.

2.2. The Thermoelectric Power

The response of a temperature sensor is governed by the difference in thermopowers of the two metal films forming the thermocouple. The calculation of the film thermopower requires the knowledge of the variation of the background relaxation time, τ_0, with energy, E, which is generally written as[30]

$$\tau_0 = \tau_b E^q \tag{15}$$

where q is a number and τ_b a constant. Moreover since the Fermi surface of metals are often non spherical[29] it is usual[29,30] to introduce the parameter

$$V = \left(\frac{\partial \ln \mathscr{A}}{\partial \ln E}\right)_{E=E_F} \tag{15}$$

which involves the aera, $\mathscr{A}$ of constant energy surfaces and thus is sensitive to distortions of the Fermi surface and the parameter

$$U = \left(\frac{\partial \ln \lambda_0}{\partial \ln E}\right)_{E=E_F} \tag{16}$$

which includes the energy dependence of the relaxation time τ_0. E_F is the Fermi energy.

The film thermopower is defined as

$$S_{fj} = S\left(\frac{d \ln \sigma_{fj}}{d \ln E}\right)_{E=E_F} \qquad j = c, m, p \tag{17}$$

with the factor S as

$$S = -\pi^2 k_B^2 T/3e E_F \tag{18}$$

where e is the absolute magnitude of the electrnic charge and k_B is the Boltzmann's constant. Hence the previous mathematical treatment leads to[14,25,31]

$$S_{fj} = S\left\{V + U\left(1 + \frac{\partial \ln F_j(\lambda_0)}{\partial \ln \lambda_0}\right)\right\}_j, \quad j = c, m, p \tag{19}$$

Introducing Eq. 11 into Eq. 19, the film thermopower can be also expressed in terms of the t.c.r. ratio[25,32]

$$S_{fj} = S\{V + U(\beta_{fj}/\beta_0)\}, \quad j = c, m, p \tag{20}$$

Taking into account that the background thermopower is given by[29]

$$S_0 = S(V + U) \tag{21}$$

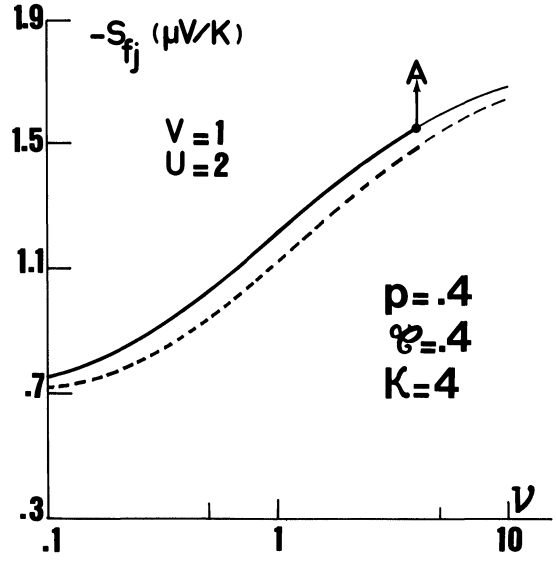

FIGURE 3 Plots of the film thermopower versus ν for $\mathscr{p} = 0.4$, $\kappa = 4$ and $p = 0.4$. The full and dotted lines are respectively for columnar and polycrystalline films (with assumed values for S of -0.632 μV/K, for V of 1 and for U of 2).

it can be seen that only the energetic parameter U is affected by the size effects due to external surface and grain-boundry scatterings. Turning to Eq. 14 these size effects cause a decrease of the absolute magnitude of film thermopower provided the physical parameters U and V have the same sign or verify the relation $|U| > |V|$. Obviously for given surface parameter, κ, and transmission coefficient, $\mathscr{p}$, this decrease must be more marked for polycrystalline and columnar films than for monocrystalline films. This feature is illustrated in Figure 3 where are represented, for $p = 0.4$, $= 0.4$, $\kappa = 4$, thermopowers of various grained films. The point A indicated in this figure is concerned with monocrystalline films in the particular case where $t = D$.

2.3. The Hall Coefficient

The sensitivity of rectangular Hall element as sensor is connected with the Hall voltage which for a thin metal film is found to be proportional to the applied transverse magnetic field and the ordinary Hall coefficient.[33] Several investigators[34–36] have detected smaller or greater variations of the Hall coefficient with decreasing film thickness than those predicted by theoretical models taking only into account the electronic scattering at external surfaces[37,38]; some of them[34,35] have suggested that these departures can be explained by assuming additional scattering at the crystalline boundaries.

Recently, some authors[39–41] have carried out the analysis for grained films. They introduce the resultant relaxation time, τ^*, in the appropriate form of the Boltzmann's equation which describes the combined action of an electric field $\vec{E}$ $(E_x, E_y, 0)$ in the plane of film and of a transverse magnetic field $(0, 0, \mathscr{B})$ (Figure 4). The mathematical treatment is then similar to the first exact analysis of surface scattering in presence of transverse magnetic field proposed by Sondheimer[37] to give the total current densities in the x- and y- directions, J_x and J_y, in the general forms

$$J_x = \frac{3}{2}\,\sigma_0(E_x\,A_j - \alpha\,E_y B_j), \quad j = c, m, p \tag{22}$$

and

$$J_y = \frac{3}{2}\,\sigma_0(E_y\,A_j + \alpha\,E_x B_j), \quad j = c, m, p \tag{23}$$

which can be easily correlated to the well known relations for perfect bulk metal satisfying the free electron model[42] if we note that the constant α

$$\alpha = \lambda_0/r \tag{24}$$

depends on the magnetic field strength by means of the radius r of the circular orbit of an electron in the magnetic field

$$r = mv.\mathscr{B}e \tag{25}$$

The effect of film structure is seen through the terms A_j and B_j which take the respective forms

$$A_j = \frac{1}{b_j}\left\{-\frac{1}{2} + a_j + \frac{\alpha^2 + b_j^2(1 - a_j^2)}{2\,b_j^2}\ln\left(1 + \frac{b_j^2(1 + 2\,a_j)}{a^2 + a_j^2 b_j^2}\right)\right.$$

$$\left. - \frac{2\,\alpha a_j}{b_j}\tan^{-1}\left\{\frac{b_j\,\alpha}{\alpha^2 + a_j b_j^2(1 + a_j)}\right\}\right\}, \quad j = c, m, p. \tag{26}$$

and

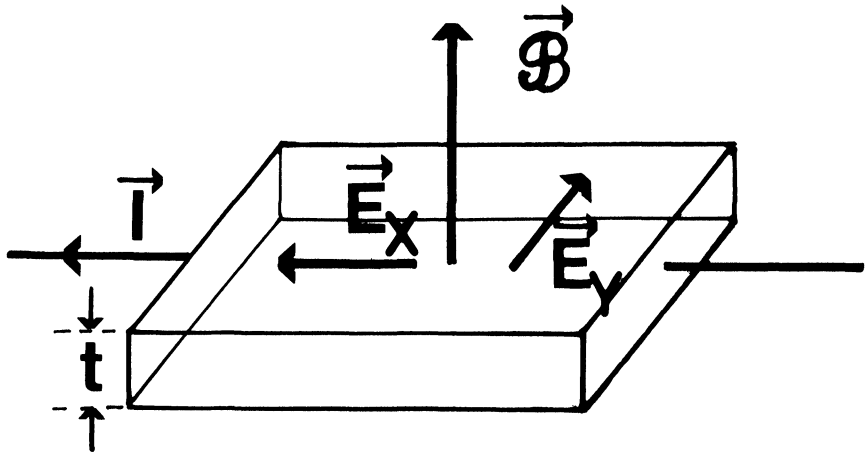

FIGURE 4 The geometry of the transverse Hall effect.

$$B_j = \frac{1}{b_j^2}\left\{-1 + a_j \ln\left(1 + \frac{b_j^2(1+2a_j)}{\alpha^2 + a_j^2 b_j^2}\right) + \frac{\alpha^2 + b_j^2(1-a_j^2)}{b_j \alpha}\right.$$

$$\left. \times \tan^{-1}\left\{\frac{b_j \alpha}{\alpha^2 + a_j b_j^2(1+a_j)}\right\}\right\}, \quad j = c, m, p \tag{27}$$

Since for the geometry of the Hall element (Figure 4) the Hall coefficient, R_{Hfj} is defined by

$$R_{Hfj} = \left.\frac{E_y}{J_x \mathscr{B}}\right|_{J_y=0} \tag{28}$$

and since in the free electron model the Hall coefficient, R_{Ho}, of the bulk material is related to the number of free electrons, n,. by the following relation[29]

$$R_{Ho} = -1/ne \tag{29}$$

the ratio R_{Hfj}/R_{Ho} of the Hall coefficient of a grained film to that of the bulk material may be written in the general form

$$R_{Hfj}/R_{Ho} = \frac{2}{3}\frac{B_j}{A_j^2 + \alpha^2 B_j^2} \quad j = c, m, p \tag{30}$$

The field strength and grain variations of the Hall coefficient can be easily computed from Eq. 30. The results are illustrated in Table 1 and Figure 5. Table 1

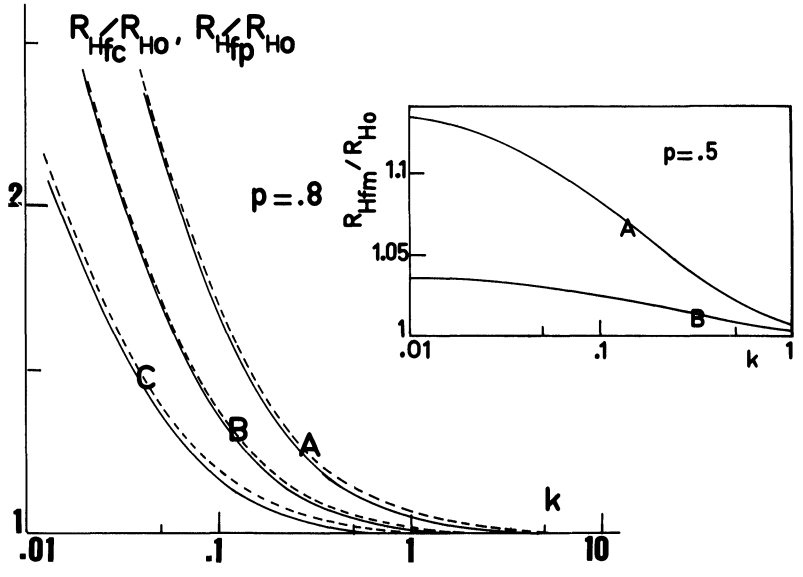

FIGURE 5 The reduced Hall coefficient R_{Hfj}/R_{Ho} with the reduced monocrystalline film thickness are shown in the inset. Curve A: $\mathscr{p} = 0.9$, Curve B: $\mathscr{p} = 0.8$.

TABLE I
Variations in the reduced Hall coefficient, R_{Hfj}/R_{Ho}, with the field parameter, α.

	Polycrystalline Films with $\nu = 1$		Monocrystalline Films with $\mathscr{C} = 0.8$, p = 0.5 and t = D	
α	$\kappa = 1$	$\kappa = 1$	k = 0.6	k = 0.06
0.01	1.02354	1.16554	1.00765	1.02877
1	1.00324	1.15760	1.00596	1.02844
10	1.00029	1.03751	1.00027	1.01369

is concerned with the variations of R_{Hfj}/R_{Ho} with the field parameter α for given polycrystalline and monocrystalline films and reveals that the strength of the applied magnetic field has almost no influence on Hall coefficient specially for monocrystalline films. Effects of external surfaces and grain structure on the Hall coefficient of grained films are illustrated in Figure 5. It can be seen that the Hall coefficient of columnar and polycrystalline films are not appreciably affected by the grain scattering process: effectively, in contrast with conductivity or thermopower behavior, the Hall coefficient of an infinitely thick polycrystalline or columnar film is equal to the bulk Hall coefficient. Moreover in the case of monocrystalline films with t = D we observe (inset of Figure 5) that the size effect in the Hall coefficient vanishes since the reduced Hall coefficient is almost equal to unity in a large range of values for the reduced thickness, $k = t/\lambda_0$, and the transmission coefficient $\mathscr{C}$ (error less than 10% for p = 0.5, $\mathscr{C} \leqslant 0.9$ and $k \geqslant 0.1$).

Hall elements operate as sensors at magnetic fields smaller than 1 T and the corresponding values of α become generally smaller than 10^{-2}. We can expand Eq. 30 in ascending powers of α and retain only terms of power 1 for low fields. This analysis leads to

$$\frac{R_{Hfj}}{R_{Ho}} \approx \frac{2}{3} \frac{g(a_j)}{[f(a_j)]^2}, \quad j = c, m, p \tag{31}$$

thus whatever is the grain structure of films the following approximate relation[43,43]

$$R_{Hfj}/R_{Ho} \approx \beta_{fj}\, \rho_{fj}/\beta_0 \rho_0 \tag{32}$$

holds in the limit of small magnetic fields.

3. ELECTROMECHANICAL PROPERTIES OF GRAINED FILMS

3.1. General Relations

The electrical resistance R_{fj} of the film is expressed as

$$R_{fj} = \rho_{fj}\, L/(wt) \tag{33}$$

where w and L are the film width and length respectively. A logarithmic differentiating of Eq. 33 gives

$$\frac{d\, R_{fj}}{R_{fj}} = \frac{d\rho_{fj}}{\rho_{fj}} + \frac{dL}{L} - \frac{dw}{w} - \frac{dt}{t} \tag{34}$$

When the substrate is bent to produce a longitudinal or a transverse strain a rigorous treatment involves[1,45-47]

i) the effect of applied strain on the background mean free path, λ_0, and the background resistivity, ρ_0. If the film material is isotropic and if the variation in λ_0 with strain $d\varepsilon$ may be entirely attributed to the change in amplitude of the thermal vibrations of atoms the strain coefficients of ρ_0 and λ_0 are given by[48]

$$d \ln \rho_0 / d\varepsilon = (\eta + 1) \tag{35}$$

$$d \ln \lambda_0 / d\varepsilon = -\eta \tag{36}$$

where the constant, η, is related to the Gruneisen's constant, $\mathscr{G}$, and to the Poisson's ratio for the film material, μ_f, by equation

$$\eta = 2\mathscr{G}(1 - 2\mu_f) \tag{37}$$

ii) the effect of applied strain on the shape of grain. In particular it is reasonable to consider the change in grain size D_i in the three x-, y- and z-directions and to write

$$dD_x/D_x \approx dL/L, dD_y/D_y \approx dw/w, dD_z/D_z \approx dt/t \tag{38}$$

If we include the influence of the substrate elasticity the well-known elasticity formulae[1,45,49,50] lead to

$$\frac{dw}{w} = -\mu_s \frac{dL}{L} \tag{39}$$

and

$$\frac{dt}{t} = -\mu_f \frac{1-\mu_s}{1-\mu_f} \frac{dL}{L} = -\mu' \frac{dL}{L} \tag{40}$$

when a longitudinal strain dL/L is applied to the substrate. μ_s is the Poisson's ratio for the substrate material.

When a transverse strain dw/w is applied to the substrate a similar analysis gives the strain equations as

$$\frac{dL}{L} = -\mu_s \frac{dw}{w} \tag{41}$$

$$\frac{dt}{t} = -\mu' \frac{dw}{w} \tag{42}$$

Then the longitudinal and transverse gauge factors of thin metallic films become

$$\gamma^*_{fLj} = \frac{dR_{fj}}{R_{fj}} \Big/ \frac{dL}{L} = 1 + \mu_s + \mu' + \gamma_{fLj} \tag{43}$$

$$\gamma^{*}_{fTj} = \frac{dR_{fj}}{R_{fj}} \Big/ \frac{dw}{w} = -1 - \mu_s + \mu' + \gamma_{fTj} \tag{44}$$

where γ_{fLj} and γ_{fTj} are respectively the longitudinal and transverse strain coefficient of film resistivity

$$\gamma_{FLj} = d \ln \rho_{fj} / d \ln L \tag{45}$$

$$\gamma_{fTj} = d \ln \rho_{fj} / d \ln w \tag{46}$$

and depend on the structure of film.

3.2. Approximate expression for the resistivity of grained films

Turning to Eq. 3 it appears that in terms of grain models the film resistivity is not explicitly expressed as a function of grain size D_x, D_y and D_z. To overcome the difficulty we can consider separately the following contributions to the total resistivity ρ_{ij}[51,52]

a) for both polycrystalline, monocrystalline and columnar films the respective contribution $\rho_{//}$ and $\rho_{\perp}$ of the strain boundaries oriented perpendicular to the applied electric field and to the y- axis which involve the respective grain parameter ν_x and ν_y.

b) For columnar and monocrystalline films, the contribution ρ^* due to background scattering and to simultaneous electron scattering at external surfaces. In the case of polycrystalline films we have to consider also the electron scattering at the grain-boundaries distributed perpendicular to the z- axis. The contribution ρ^* is described by a scattering parameter, ξ_j, which is given by

$$\xi_p^{-1} = \kappa^{-1} + \nu_z^{-1} \tag{47}$$

for polycrystalline films and reduces to

$$\xi_j = \kappa^{-1} \quad j = c, m \tag{48}$$

for monocrystalline and columnar films.

Assuming that the resistivities $\rho_{\perp}$, $\rho_{//}$ and ρ^* are additive a general approximate form for the total film resistivity is

$$\rho_{fj}/\rho_0 = [F(\nu_x)]^{-1} + [G(\nu_y)^{-1} + [G(\xi_j)]^{-1} - 2 = M_j(\nu_i, \kappa) \quad j = c, m, p \tag{49}$$

where

$$G(\xi) = \frac{3}{2} \xi \cdot f(\xi) \tag{50}$$

and

$$F(\nu) = 3\nu\left[\frac{1}{2} - \nu + \nu^2 \ln(1+\nu^{-1})\right] \tag{51}$$

Provided that grain boundaries and external surfaces act as moderately efficient scatterers ($\kappa > 0.4$, $\nu > 0.4$) reasonable deviations from the previous grain model are obtained.[51] Thus Eq. 49 seems convenient to perform the calculations of strain coefficients of grained films.

3.3. Strain Coefficients of Resistivity of Grained Films

Logarithmic differentiation of Eq. 49 gives after some mathematical manipulations

$$\frac{d\rho_{fj}}{\rho_{fj}} = \frac{d\rho_0}{\rho_0} - \frac{1}{M_j}\left\{\frac{1}{F^2(\nu_x)} \cdot \frac{dF(\nu_x)}{d\nu_x} + \frac{1}{G^2(\nu_y)} \cdot \frac{dG(\nu_y)}{d\nu_y} + \frac{1}{G^2(\xi_j)} \cdot \frac{dG(\xi_j)}{d\xi_j}\, d\xi_j\right\} \quad j = c, m, p \tag{52}$$

Turning to the definitions of surface parameter, κ, and grain parameter, ν_i, it yields

$$\frac{d\nu_i}{\nu_i} = \frac{dD_i}{D_i} - \frac{d\lambda_0}{\lambda_0}, \quad i = x, y, z \tag{53}$$

$$\frac{d\kappa}{\kappa} = \frac{dt}{t} - \frac{d\lambda_0}{\lambda_0} \tag{54}$$

Then from Eqns (47) and (48) we obtain

$$\frac{d\xi_p}{\xi_p} = \xi_p\left[\frac{d\kappa}{\kappa} \cdot \frac{1}{\kappa} + \frac{d\nu_z}{\nu_z}\frac{1}{\nu_z}\right] \tag{55}$$

and

$$\frac{d\xi_j}{\xi_j} = \frac{d\kappa}{\kappa}, \quad j = c, m \tag{56}$$

Defining for convenience the functions

$$F^*(\nu) = \nu \cdot \frac{dF(\nu)}{d\nu} \cdot [F(\nu)]^{-2} \tag{57}$$

with

$$\frac{dF(\nu)}{d\nu} = \frac{3}{2} - 6\nu + 9\nu^2 \ln(1+\nu^{-1}) - \frac{3\nu^2}{1+\nu} \tag{58}$$

and

$$G^*(\xi) = \xi \frac{dG(\xi)}{d\xi} [G(\xi)]^{-2} \tag{59}$$

with

$$\frac{dG(\xi)}{d\xi} = \frac{3}{2} (3\xi - \frac{3}{2} + (1 - 3\xi^2) \ln(1 + \xi^{-1})) \tag{60}$$

Introducing Eqs (38) to (40) and (53) to (60) into Eq. (52) the longitudinal strain coefficient γ_{fLj} is found to be

$$\gamma_{fLj} = (\eta + 1) + M_j^{-1} [-(\eta + 1) F^*(\nu_x) + (\mu_s - \eta) G^*(\nu_y) + (\mu' - \eta) G^*(\xi_j)],$$

$$j = c, m, p \tag{61}$$

In a similar way the transverse strain coefficient, γ_{fTj} takes the form

$$\gamma_{fTj} = (\eta + 1) + M_j^{-1} [(\mu_s - \eta) F^*(\nu_x) - (\eta + 1) G^*(\nu_y) + (\mu' - \eta) G^*(\xi_j)],$$

$$j = c, m, p \tag{62}$$

Eqs (61) and (62) are simple analytical expressions which satisfy essential physical requirements:

i) When the electronic scattering at grain boundaries becomes negligible the transverse and longitudinal strain coefficient reduce to a similar expression

$$\gamma_{fL}, \gamma_{fT} = (\eta + 1) + (\mu' - \eta) G^*(\kappa) \tag{63}$$

which agrees with the epxression deduced from the Cottey model.[53]

ii) When the electronic scattering at external surfaces vanishes, i.e. when $t \to \infty$ or when $p = 1$, Eqs (61) and (62) tend to limiting values, γ_{gLj} and γ_{gTj}, which depend only on the grain parameter ν_i. Note also that for monocrystalline films strain coefficients reduce to the background coefficient, $\eta + 1$, since an infinite film thickness implies infinite grain sizes D_i.

Figure 6 represents the thickness dependence of strain coefficients, γ_{fLm} and γ_{fTm}, of monocrystalline films when the film thickness, t, is exactly equal to grain sizes D_i and in the particular case of silver film ($\mu_f = 0.38$, $\eta = 1.15$) deposited on a glass substrate ($\mu_s = 0.25$). Comparison with the Cottey result (curve A) shows that for monocrystalline films the main grain-boundary effect is to enhance the overall size effect.

Variations in columnar film strain coefficients, γ_{fLc} and γ_{fTc}, are shown in Figure 7 assuming as usual that grain sizes measured in the x-, y- and z- direction take equal values ($\nu_x = \nu_y = \nu$). Figure 7 reveals several interesting features.

i) By comparison of Figure 7 with Figure 6 it appears that for large values of the grain parameter, ν, the plot of variations in the strain coefficient versus the surface parameter κ approaches the Cottey plot.

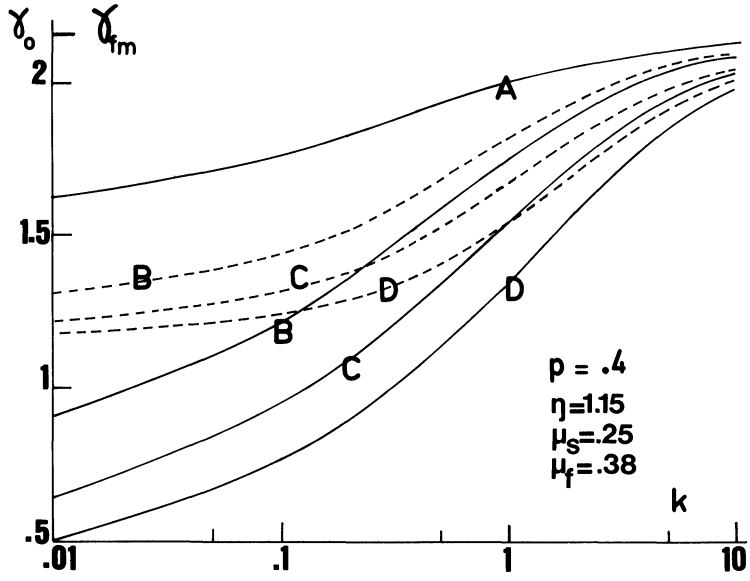

FIGURE 6 Variations in the strain coefficient of thin monocrystalline films, γ_{fLm} (full lines) and γ_{FTm} (dotted lines), with the reduced thickness, k, for p = 0.4. Curve A: Cottey's curve, Curve B: $\mathscr{E}$ = 0.8, Curve C: $\mathscr{E}$ = 0.6, Curve D: $\mathscr{E}$ = 0.4.

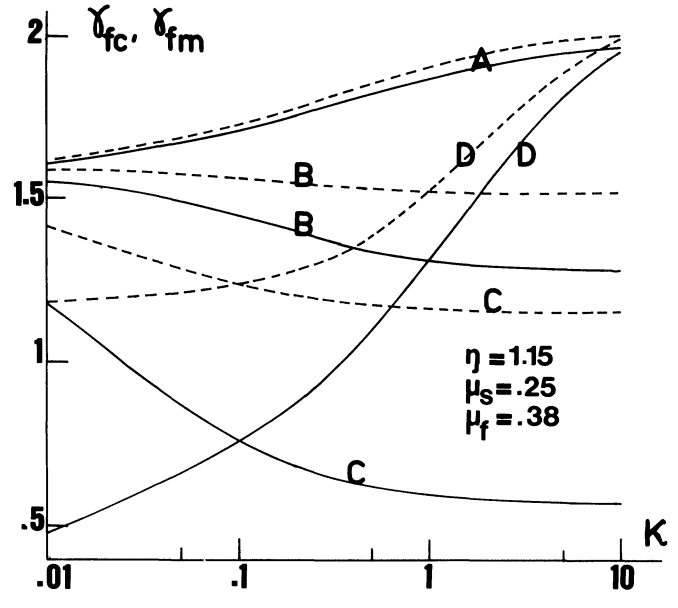

FIGURE 7 Variations in the strain coefficients of columnar films, γ_{fLc} (full lines) and γ_{fTc} (dotted lines), with the surface parameter κ. Curve A: ν = 10, curve B: ν = 1, curve C; ν = 0.1. Curve D are concerned with monocrystalline films with values for p of 0.4 and for $\mathscr{E}$ of 0.4.

ii) In the limit of large values of the surface parameter the strain coefficients reduce to asymptotic values γ_{gLc} and γ_{gTc} which markedly depend on the grain parameter.

iii) The size effects in strain coefficients of columnar films are dominated by the scattering at grain boundaries; in particular it can be seen that the size effect corresponds either to an increase or to a decrease in strain coefficients according to the value of the grain parameter.

iv) To allow an easy comparison of grain boundary effects in columnar films with effects in monocrystalline films (with D = t) a plot concerned with such monocrystalline films is also reported in Figure 7. It appears that size effects due to simultaneous grain boundary and external surface scatterings are less pronounced in columnar films than in monocrystalline films.

iv) Care must be taken that, according to definitions of columnar and monocrystalline films any curves A to E in Figure 7 should correspond, for increasing κ, to films exhibiting successively a monocrystalline structure with constant grain sizes $D_i > t$ and a columnar structure with $D_i < t$.

The curves illustrating the thickness dependence of strain coefficients of polycrystalline films are similar to the curves shown in Figure 7. These curves have been well discussed in several papers[14,46,47] and for this reason are not reported here. However it should be pointed out that for a given value of the surface parameter, strain coefficients of resistivity in polycrystalline films are always smaller than strain coefficients of resistivity in columnar films as shown in Figure 8.

At this point it may be of interest to consider the influence of the grain structure on the cross sensitivity K defined as

$$K = \gamma^*_{fTj}/\gamma^*_{fLj} \tag{64}$$

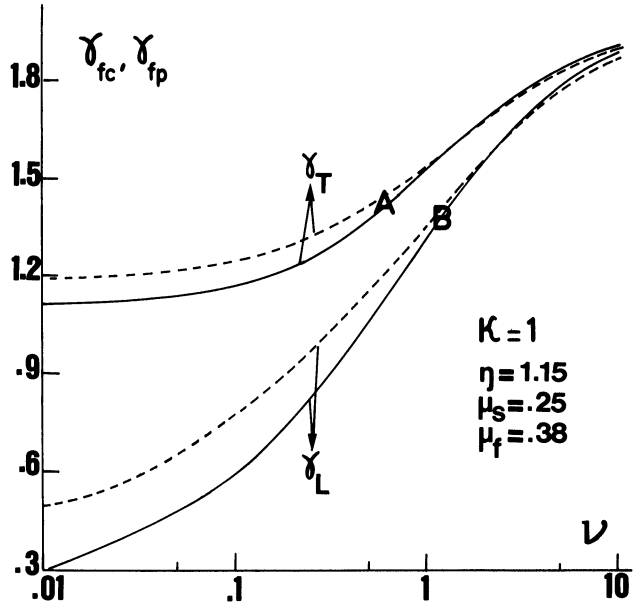

FIGURE 8 Variations in the strain coefficients of columnar (full lines) and polycrystalline (dotted lines) films with the grain parameter ν for $K = 1$.

Effectively if the lateral dimenion of a strain gauge is not negligible in comparison with its length the gauge becomes sensitive to transverse strains. The cross sensitivity constitutes a measure of this spurious effect. For a supported longitudinal strain gauge we obtain the real gauge factor as

$$\gamma^*_{Lr} = \gamma^*_{fLj}(1 - \mu_s K) \tag{65}$$

thus the correction factor is found to be directly proportinal to the cross sensitivity.

Table 2 shows that the main effect of grain boundary scattering is to reduce the theoretical cross-sensitivity of strain gauge by a factor of about 30%.

4. THIN METAL FILMS AS SENSORS

The purpose of this section is to discuss the possible development of thin metal film sensors in terms of theoretical results presented in previous sections. Emphasis is placed in particular on temperature effects but some indications on possible effects of grain structure on range of operation and temporal stability are also given.

4.1. Temperature Sensors

4.1.1. Film resistors Thick metal films, specially platinum metal films[5,54,55], are now commonly used in the development of transducers for accurate surface temperature measurements. In most cases these temperature sensors produced by photochemical process[55] are glued on the surface. Thus the bonding technique and specially the choice of cement used for bonding the sensor to the test surface are of prime importance for reproducibility over a specified temperature range. To avoid these difficulties the metal film can be deposited directly on the test surface. In particular, copper which is useful over temperature ranges of 125 K to 420 K can be easily prepared by vacuum evaporation or sputtering. The copper film resistivity and t.c.r. depend upon impurities, thickness but also mainly upon grain structure.

Grain boundary scattering can drastically decrease the film t.c.r. Consider the case of a polycrystalline copper film 1 μm thick with small grain size ($D/\lambda_0 = 0.4$) and weak transmission coefficient ($\mathscr{C} = 0.4$) a t.c.r. ratio β_{fp}/β_0 of about 0.25 is predicted. Then films exhibiting a monocrystalline structure are desirable. The formation of monocrystalline films is primarily a question of deposition method and of substrate temperature.[15,22,56,57] Thermal aging which generally results in grain-growth[15,18,57–60] can markedly improve the performance of thin metal film resistors.

Thick film as well as thin film resistors are sensitive to mechanical strains as well as to thermal strains caused by the thermal mismatch between the film and its substrate. Thermal strains in supported films are expressed as[61]

$$\epsilon_i = (\alpha_s - \alpha_f)(T - T_R) \quad i = x, y \tag{66}$$

TABLE II

The cross sensitivity of grained films with the assumed values for η of 1.15, for μ_s of 0.25 and for μ_f of 0.38. The cross sensitivity for perfect bulk metal is equal to 0.352.

	Polycrystalline films		Columnar films		Monocrystalline films for p = 0.4		
K	$\nu = 4$	$\nu = 4$	$\nu = 4$	$\nu = 4$	k	$\mathscr{C} = 0.4$	$\mathscr{C} = 0.8$
0.1	0.221	0.267	0.219	0.267	0.1	0.181	0.221
1	0.209	0.292	0.201	0.292	1	0.247	0.298
10	0.206	0.303	0.199	0.308	10	0.331	0.344

$$\epsilon_z = -2[\mu_f/(1-\mu_f)]\,(\alpha_s - \alpha_f)\,(T - T_R) \tag{67}$$

where α_s and α_f are the coefficients of linear expansion of substrate and film, respectively and T_R is a reference temperature. Since the thermal expansion coefficients, α_f and α_s, lie generally between 3.10^{-5} and 3.10^{-6} K^{-1} [20] thermal strains can markedly exceed 10^{-2} for a deviation of temperature from T_r of 300 K. Thus, as suggested by some authors[32] the correcting term of prime importance in the theoretical formulation of supported film t.c.r. is the correcting term due to thermal strains even if the strain coefficients of resistivity are generally lower for grained films than for the perfect bulk material and consequently if grained film will exhibit a better mechanical and thermal strains stability.

Moreover vacuum deposited films are frequently in a state of intrinsic stresses. The intrinsic stress is due to the accumulating effect of the crystallographic flows that are built into the film during deposition.[20] Intrinsic stresses are sensitive to the deposition conditions and specially to the substrate temperature, T_s, during condensation.[20,57] Let be T_m the melting point of film material. It has been shown that for low melting point metals such as $T_s/T_m > 0.2$ thermal recovery tends, by bulk diffusion, to relax intrinsic stresses[20] but for high melting point metals deposited at low temperatures intrinsic stresses accumulate and tend to dominate over thermal stresses. Consider the case of copper films ($T_m = 1353$ K) the substrate during deposition must be kept at temperature higher than 271 K; this condition can be easily fulfilled. However in the case of platinum ($T_m = 2043$ K) films must be evaporated in bringing the substrate to temperature higher than 400 K to prevent accumulating intrinsic stresses. Moreover for evaporated and annealed films intrinsic tensile stresses attributed to grain structure increase with film thickness[20,57] and result in poor adhesion. Thus at the light of these results the tendency must be to develop moderately thick film sensors.

4.1.2. Thin film thermocouples The use of thin metal film thermocouple devices which have small thermal capacity and fast response time of the order of 10^{-6} s has greatly increased in measurements of surface temperature. They provide as thin film resistors the advantage of intimate thermal contact with the surface. Several workers[62–66] have investigated the thermoelectric properties of thin film thermocouples constructed from nickel, iron, copper, molybdenum, constantan and chromel. In general the thermoelectric properties of thin film thermocouples are found to depend markedly on the purity and the structure of the vacuum deposited elements.[14,62,63,65] The purity of the deposition source presents a great interest if the main application of the thermocouple is in the measurement of low temperatures since impurities affect the low temperature thermopower of materials drastically. Effectively according to the Wiedeman-Franz's Law[30] the total thermopower, S*, of the film is expressed as

$$S^* \rho^* = \rho_{fj} S_{fj} + \rho_I S_I \quad j = c, m, p \tag{68}$$

where S_I and ρ_I are respectively the thermopower and the resistivity due to impurity atoms frozen in the film and ρ^* is the total resistivity satisfying the Matthiessen's rule.[29]

In most cases the thermopower of metal film elements[12–14,36,67–71] as well as the thermal emf in thin film couples[62,63,65] exhibit marked thickness and structural defects effects. Annealing causes a marked decrease of these effects[12,36,62,68–71] and after subsequent thermal annealing the film material thermopower is generally found to be below the bulk value.[12–14,36,38] Since annealing results mainly in mechanical reordering of the top surface[72–76] and grain growth[15,18,57,60] the observed results can be easily understood in terms of size effects due to both grain-boundary and external surface scatterings.

The thermocouple output may be written to the first approximation as[5,66]

$$\theta = (S_{fj}^{A} - S_{fj}^{B})\,\Delta T \tag{69}$$

where the superscript A and B refer respectively to the materials forming the thermocouple. As discussed in previous section, efficient grain boundary scattering can result in a pronounced reduction in film thermopowers depending upon the sign and upon the absolute magnitude of the energetic parameters U and V. But as the transducer response involves the difference in thermopowers this decrease may be weakly less marked if the couples are made from two materials whose thermopowers, S^A and S^B, have the same sign. Improvement of the temperature sensitivity of thin film thermocouples can be reasonably expected from an accurate choice of film materials which determines the energetic parameters U and V and from suitable preparation and annealing techniques.

At this point it might be of interest to remark that grain boundaries constitute dominant short circuit paths for diffusion in thin films.[15] Hence at high annealing temperatures a transition layer can be formed by diffusion of the two element materials of the thermocouple which can affect the temporal stability as well as the temperature sensitivity of temperature sensors. In these conditions the high temperature range of operation of thin film thermocouples must be considerably reduced if necessary.

It is also desirable to prepare thin film elements characterized by an homogeneous structure. Effectively if grains grow in different ways inside thin films in addition spurious thermal emfs can be generated which vary with time. Moreover inhomogeneous grain structures are also responsible of tensile stresses[20] which will age specially with temperature variations.

Bulk thermocouples as well as thin film thermocouples are stress sensitive. However the theory predicts that in thoroughly annealed and homogeneous grained films mechanical and thermal strain effects are reduced with respect to those in the bulk. Care must be also taken the theoretical relation[20] is not exactly verified in experiments since it corresponds to unsupported films. Some authors[77] have proposed a general expression for the thermoelectric power of grained films attached on a substrate. The correcting terms due to thermal expansions of the film and its substrate are calculated including thermal strains. Comparison with experiments shows that in the case of noble metals the more important correction is due to thermal strains. In most cases, these correcting terms lead to deviations less than 5% so that theoretical predictions of Eq. 20 cannot be rigorously confirmed experimentally.

4.2. Hall Effect Sensors

Theoretical studies of the Hall effect in thin grained metal films have provided evidence that the response of thin-film Hall elements is not affected by grain boundary scattering effects. Moreover thin grained metal films are expected to be superior to conventional semiconductor Hall devices in their magnetic field strength independent sensitivity.

However it should be pointed out the relation[29] derived in terms of the free electron model constitutes a rough approximation. Effectively the "density of carriers" n which appears in Eq. 29 is in reality a complicated function of the states at the Fermi surface[29] so that as thermopower the Hall coefficient is a sensitive function of the shape of the Fermi surface.[29,33] Values of the Hall coefficient for various metal films reported by various authors[34-36,78-82] are not always in agreement with theoretical predictions of section 2.3. In particular, the Hall coefficient of films was found to be lower or considerably greater than that predicted by size effect theories.[34-36,78-81] A reversal of sign of the Hall coefficient was also observed.[81,82]

Some attempts have been made to interpret the observed behavior in terms of high concentrations of lattice defects[36,79,80] such as vacancies or dislocations which cause distortions of the Fermi surface as well as in terms of high concentration of impurities.[80,82] At any given concentration of impurities the Hall coefficient will be given by an expression concerned with a two band model[33] involving two separate relaxation times. Any relaxation time associated to each scattering mechanism has its own anisotropy so that when the impurity scattering is the dominant scattering process the Hall coefficient changes from its bulk values and dependent on the nature of impurites reverses its sign.[33]

As thermal agings at temperature T_A modify strongly the concentration of point defects, changes in Hall coefficient will be marked. Thus we might also mention that the Hall element will not further operate at temperatures higher than T_A in order to leave the sensor response unaltered.

In homogeneous and thoroughly annealed then grained films, however, it is reasonable to expect the agreement with multi-dimensional model to be rather good. Since the sensitivity of the Hall element is defined as the ratio, $V_H/\mathscr{B}\,I$, of the Hall voltage V_H over the product control current, I,. magnetic field, $\mathscr{B}$, the sensitivity of grained metal films will be considerably small compared with the sensitivity of semiconductor films. The sensitivity of metallic Hall element is at room temperature typically 10^5 time less than the sensitivity of InAs Hall sensors. However if the thermal stability of the Hall element is of prime importance during operation it is obvious that the exponential dependence on temperature of the free carrier density gives to semiconductor devices a thermal sensitivity too large to use such devices over large temperature range without marked deviations from ideal behavior. In contrast thin metal film devices offer the advantage of a good thermal stability. Effectively in metal films in which external surfaces act as efficient scatterers and which exhibit nearly linear R_H versus T plot it is possible to derive a theoretical expression for the temperature coefficient β_{RH} of Hall coefficient defined as

$$\beta_{RH} = d\ln R_{Hf}/dT \tag{70}$$

Since both the bulk mean free path, λ_0, and the electronic density, n, vary with temperature it yields after some calculations[83,84]

$$\beta_{RH} = -\beta_n - \beta_0\, F(\kappa) \tag{71}$$

where β_n is the temperature coefficient of the electronic density defined as

$$\beta_n = d\ln n/dT \tag{72}$$

The function $F(\kappa)$ depends on the surface parameter, κ, in such a way that when κ reaches 1, $F(\kappa)$ takes values as low as -0.043. It thus appears that $\beta_0 \times F(\kappa)$ does not usually exceed $10^4\ K^{-1}$. Hence the temperature coefficient β_{RH} is essentially determined by thermal variations in the electronic density which for metals are known to be particularly low.[29] In contrast for semiconductor Hall sensors widely used for commercial applications such as thin film In As or In Sb Hall elements the temperature coefficient of resistivity is respectively about $2.10^{-3}\ K^{-1}$ and $2\ 10^{-2}\ K^{-1}$ whereas between 273 and 323 K the temperature coefficient of the Hall voltage reaches respectively $10^{-3}\ K^{-1}$ for InAs films and $10^{-2}\ K^{-1}$ for InSb films. Moreover provided the magnitude of β_n is less than that of β_0 small variations in the Hall coefficient of grained metal films with temperature can be reasonably predicted. Effectively if we turn to theoretical treatments devoted to films in which the grain boundary scattering is respectively efficient and negligible. Hence, in general, thin metal films should yield low value of the temperature

coefficient of sensitivity (typically less than 10^{-4} K^{-1}).

At last, temporal stability of thin metal film Hall elements is, as discussed in previous section, essentially determined by the efficiency of the annealing process; high temperature process as well as the use of protective coating over the surface of Hall elements constitute suitable technique in the production of stable Hall sensors.

4.2. Thin Film Strain Gauge

It is the aim of this section to discuss the advantage and disadvantage of using as strain devices thin grained films whose transport properties can be interpreted in terms of multi-dimensional models of grain boundaries. Hence some conclusions brought here will present some analogies with conclusions reported in a previous paper[45] devoted to the electromechanical properties of films described by the Mayadas-Shatzkes model.[85]. The main difference between these two discussions arises from the geometry of the two models. The Mayadas-Shatzkes model is essentially a uni-dimensional model,[14] consequently in calculations only changes with applied strain of the grain size lying in the direction of the applied electric field are considered. Hence theoretical results on variations of strain coefficients of resistivity with thickness and grain parameters as obtained in the framework of multi-dimensional models will differ from results concerned with the Mayadas-Shatzkes model.

A quantitative understanding of the effect of film structure on the strain sensitivity of thin metal films is easy from the data of figures 6 to 8. It is interesting to comment some features:

i) In the case of relatively thick monocrystalline films the strain sensitivity is not seriously altered by grain-boundary scattering and as long as we are concerned with the strain sensitivity, thick monocrystalline films behave as bulk material.

ii) In the case of columnar and polycrystalline films the situation is not equivalent; in particular reversal of the size effect can be caused by dominant grain-boundary scattering process. In absence of knowledge of the shape and the size of grains it is not possible to predict easily the electromechanical behavior of columnar or fine-grained films. When very efficient grain-boundary scattering process is present it is preferable to avoid a marked reduction of the strain sensitivity to keep the strain devices relatively thin.

Thus columnar and polycrystalline films should exhibit a poor strain sensitivity but in addition, as indicated in section 3, the cross sensitivity of strain devices should be much less marked than for bulk strain devices.

In practice thermal stability is a considerable problem in thin film strain devices. In general a low TCR material in film devices is required. Effectively we can define a temperature coefficient of the gauge factor as

$$\beta\gamma_{fj}^{*} = \mathrm{d} \ln \gamma_{fj}^{*}/\mathrm{dT} \tag{73}$$

Turning to Eqs (43) and (44) it yields[1,86]

$$\beta\gamma_{fj}^{*} = -\beta_{fj}^{*} + \frac{1}{R_{fj}} \frac{\partial}{\partial T} \left(\frac{\partial R_{fj}}{\partial \epsilon} \right)_{T} \tag{74}$$

where β_{fj}^{*} is the temperature coefficient of resistance (TCR) of the film including the linear expansion of the film. In general the value of β_{fj}^{*} does not markedly from the t.c.r., β_{fj}, value.[14,87]

The second term into Eq. (74) takes into account the effect of a thermal mismatch between the film and its substrate which gives rise to thermal strains.[1,5,14] Experimental works on metal films in the thickness range 300 to 1300 have established that $(\partial R/\partial \varepsilon)_T$ is independent of temperature.[88] It now seems that changes in gauge factor, γ_{fj}, with temperature are predominantly determined by the film TCR. As a consequence, as outlined in a previous paper,[45] it might be expected that the gauge factor of polycrystalline and columnar films would exhibit a low temperature coefficient. Turning to the example of a columnar film with $\nu = 1$ and $\kappa = 1$, the grain-boundary effect results, with respect to bulk values, in a decrease of about 35% for the longitudinal gauge factor together with a correlated decrease of the film TCR of about 100%. Thus the poor strain sensitivity of thin polycrystalline and columnar films is counterbalanced by a good thermal stability.

The stability of strain gauges with time is governed by factors discussed in previous paragraphs such as the inhomogeneity of film structure which gives rise to intrinsic stresses. Grain-boundary diffusion which occurs in badly annealed films and electromigration failure[15,89] which happens when grain sizes change abruptly from small to large can seriously alter the temporal stability of strain devices operating over large temperature range. Annealing which results in grain growth and annihilation of small grains is a remedy to both intrinsic stresses and electromigration failure. Also surface passivation reduces electromigration considerably[15] by reducing vacancy formation and inducing grain growth during glassing at very high temperatures.

4.4. Gas Sensors

Actually solid state gas sensors consist, essentially, of semiconductor gas sensors which are usually based on the surface properties of ZnO[90,91] or SnO_2[92–95] films. Special semiconductor films such as phthalocyanine films[96] are suitable for selective gas detecting systems. The advantage of this form of sensors is to respond with a high sensitivity[90,94–96] to the presence of ambiant combustible gases in low ppm concentration. The disadvantages include non linearity and sensitivity to ambiant temperature.[92,93,95]

Thin metal films as gas sensors will present the advantage of small size together with low thermal sensitivity. Hence, the purpose of this section is at the light of previously published results to prospect possible applications of thin metal films as gas sensors.

Several experimental works[97,101] have given evidence that the electrical resistance of thin metal films changes during the adsorption of gas molecules. Investigation by Wedler and co-workers[97,100] of the adsorption of carbon monoxide on nickel and copper films has revealed changes in the resistivity as high as 20%. Moreover, the resistance increase has been found to vary inversely as the film thickness. This result agrees with results on the resistivity change caused by adsorption of 1% atoms O_2 on Au films.[98] Surplice et al[99] studied the adsorption of)$_2$ on E_r and T_i films; increase of the resistance of about 42% to 20% was observed. However in the thickness range investigated (200 to 400 Å) the observed increase of resistance was roughly proportional to the film thickness in contradiction with data concerned with other film materials. Furthermore the long-term stability and reproducibility of gas response has not yet clarified. Study of desorption on system Au/O[98] showed a small irreversibility of the resistivity changes. But Borodziuk-Kulpa et al reported[101] significant and irreversible changes in the film t.c.r. induced by gas absorption process.

It thus appears that some of the main parameters of thin film sensors such as gas selectivity, linearity and reproducibility of the response are not actually well investigated but thin metal films can perhaps constitute interesting applications in gas detection specially in measurements of very small concentrations of gas.

Another interesting possibility is to make use of the large change in Hall effect in metal films caused by gas chemisorption.[100,102,103] For example the influence at 77 K of the adsorption of CO on the Hall coefficient of thin Cu films (200 Å thick) was studied by Wedler et al.[100] A marked decrease (about 20%) of the Hall coefficient was observed for a monolayer of adsorbed CO. More interesting are the results reported by Bastl[103] which showed that hydrogen chemisorption causes a large change in the value of the Hall coefficient of a 110 Å thick Tungsten film (about 30% when the surface coverage by hydrogen atoms reaches 0.75). Moreover the dependence of the Hall coefficient on the surface coverage was found to be linear.

Such results seem at first sight promising but on the basis of published data it appears that more effort both theoretically and experimentally are required to obtain a realistic picture of the possibilities of extending without doubt thin metal film sensors to gas sensing problems.

5. CONCLUSION

The main transport parameters of grained thin metal films are found to depend markedly on the grain structure of film and weakly on the film thickness. Hence the grain-boundary scattering can affect greatly the response of thin metal film sensors based on the thermoelectric effect, strain effects or variations in the film resistivity with temperature. Theoretical models show that the Hall effect alone is not altered by grain-boundary scattering. In general, the sensitivity of the metal film sensor is reduced by grain-boundary effects. It is not possible to decide, in a general way, what thickness or grain structure is preferable for metal film sensors; the response to this question depends on the application of the metal film sensor and on the environment specially on the environmental temperature influence. For example, thin metal resistors must be formed preferentially from moderately thick monocrystalline films whereas thin columnar or polycrystalline films with grain parameter $\nu \simeq 1$ would be particularly desirable for strain gauges operating in a tough temperature environment.

It must be pointed out that the thermal stability of grained film sensor is in general markedly improved with respect to that of perfect bulk metal sensors provided grained films are thoroughly annealed.

Effectively deposition conditions as well as annealing conditions are of prime importance in improvement of the response of thin metal films sensors. By accurate choice of the deposition parameters it is possible to prepare homogeneous films and thus to develop sensors with improved long-term stability. At the light of Section 4 a specified annealing procedure which results in annihilation of point defects and in grain growth is needed in order to relax intrinsic stresses and to avoid bulk diffusion processes and consequently in order to provide a good reproducibility and reliability of film devices.

The field of applications of thin metal film sensors which present the advantages of small size, good thermal stability and intimate contact with the test surface seems promising. But the possibility of progress in the development of high performance film sensors is primarily determined by the development of suitable deposition and aging techniques and of additional structure analysis techniques.

REFERENCES

1. G.R. Witt, *Thin Solid films*, **22** (1974) 133–156.
2. M. Desjardins "Les Capteurs de Mesure", (La Documentation Française, Paris, 1975) p. 60.
3. J. Goualt, M. Hubin, G. Richon and B. Eudeline, *Symp.* Capteurs Française (CIAME, Paris, 1976) 29–33.

4. A.J. Tosser, C.R. Tellier and C.R. Pichard, *1st Int. Conf. on Applied Modeling and Simulation* (Lyon, France, September 1981) Vol II, 63-67.
5. G. Asch "Les capteurs en Instrumentation Industrielle", (Dunod, Paris, 1981) Chapter 6 and 7.
6. T.G.M. Kleinpenning, *Sensors and Actuators*, **4** (1983) 3-9.
7. P. Daniil and E. Cohen, *J. Appl. Phys.*, **53** (ii) 8257-8259.
8. P.H. Mansfield "Electrical transducers for industrial measurement", (Butterworths, London, 1973) p. 154.
9. A. Bryant, M. Poirier, G. Riley, D.L. Lee and J.V. Vetelino, *Sensors and Actuators*, **4** (1983) 105-111.
10. S.J. Raeburn and R.V. Aldridge, *Phys. Lett.*, **63 A** (1977) 66-68.
11. P.M. de Groot, *These Doctorat ès Sciences*, (University of Grenoble, France, 1980).
12. G. Wedler and R. Chander, *Thin Solid Films*, **65** (1980) 53-60.
13. See for exmaple, K.L. Chopra "Thin film phenomena", (McGraw-Hill, New York, 1969).
14. See for example, C.R. Tellier and A.J. Tosser, "Size effects in thin films", (Elsevier, Amsterdam, 1982).
15. S.D. Mukherjee in "Reliability and degradation", M.J. Howes and D.V. Morgan, Eds, (John Wiley Sons, Chichester, 1981) Chapter 1.
16. R. Abermann and R. Koch, *Thin Solid Fioms*, **66** (1980) 217-232.
17. H.T.G. Nilsson, B. Andersson and S.E. Karlsson, *Thin Solid Films*, **63** (1979) 87—92.
18. K. Uda, Y. Matsuchita and S.I. Takasu, *J. Appl. Phys* **51** (1980) 1039.
19. M. Murakami, *Thin Solid Films*, **59** (1979) 105-116.
20. J.A. Thornton, D.W. Hoffman, Technical Report n° 79 135 (1979) (U.S.A.).
21. K. Kinosita, *Thin Solid Films*, **12** (1972) 17-28.
22. P. Petroff, T.T. Sheng, A.K. Sinha, G.A. Rozgonyi and F.B. Alexander *J. Appl. Phys.*, **6** 2545- 2554.
23. S. Sen, R.K. Nandi and S.P. Sen Gupta, *Thin Solid Films*, **48** (1978) 1-16.
24. C.R. Tellier, C.R. Pichard and A.J. Tossr, *Thin Solid Films*, **61** (1979) 349-354.
25. C.R. Tellier and A.J. Tosser, *Thin Solid Films*, **70** (1980) 225-234.
26. C.R. Pichard, C.R. Tellier and A.J. Tosser, *Thin Solid Films*, **62** (1979) 189-194.
27. E.H. Sondheimer, *Adv. Phys.*, **1** (1952) 1-50.
28. C.R. Pichard, C.R. Tellier and A.J. Tosser, *Phys. Stat. Sol. (a)*, **65** (1981) 327-334.
29. J.M. Ziman "Electrons and phonons", (Oxford University Press, London, 1962).
30. R.D. Barnard, "Thermoelectricity in metals and alloys", (Taylor and Francis, London, 1972) Chapters 2, 3 and 6.
31. L. Ouarbya, C.R. Tellier and A.J. Tosser, *J. Mater. Sci.*, **16** (1981) 2287-2289.
32. C.R. Pichard, A.J. Tosser and C.R. Tellier *J. Mater. Sci.*, **17** (1982) 10-16.
33. C.M. Hurd, "The Hall effect in metals and alloys" (Plenum Press, 1972) Chapters 1, 2 and 3.
34. K.L. Chopra and S.K. Bahl, *J. Appl. Phys.*, **38** (1967) 3607-3610.
35. V.P. Duggal and V.P. Nagpal, *J. Appl. Phys.*, **42** (1971) 4500-4503.
36. R. Suri, A.P. Thakoor and K.L. Chopra, *J. Appl. Phys.*, **46** 91975) 2574-2582.
37. E.H. Sondheimer, *Phys. Rev.*, **80** (1950) 401-406.
38. C.R. Tellier, M. Rabel and A.J. Tosser, *J. Phy. F: Metal Phys.*, **8** (1978) 2357-2365.
39. C.R. Pichard, A.J. Tosser and C.R. Tellier, *Thin Solid Films*, **69** (1980) 157-164.
40. C.R. Pichard, A.J. Tosser and C.R. Tellier, *J. Mater. Sci.*, **16** (1981) 451-456.
41. C.R. Pichard and A.J. Tosser, C.R. Tellier, K.C. Barua, *J. Mater. Sci.*, **16** 91981) 2480-2484.
42. F.S. Blatt, "Physics of electronic conduction in solid" (McGraw-Hill, New York, 1968) Chapter 7.
43. C.R. Pichard, C.R. Tellier and A.J. Tosser, *J. Phys. F: Metal Phys.*, **10** (1980) L101-L103.
44. C.R. Pichard, C.R. Tellier and A.J. Tosser, *Phys. Stat. Sol. (a)*, **68** (1981) K 171 - K 125.
45. C.R. Tellier and A.J. Tosser, *Electrocomp. Sci. & Technol.*, **4** (1977) 9-17.
46. C.R. Pichard, C.R. Tellier and A.J. Tosser, *J. Mat. Sci.*, **15** (1980) 2991-2994.
47. C.R. Tellier, C.R. Pichard and A.J. Tosser, *J. Mat. Sci.* **16** (1981) 2281-2286.
48. G.C. Kuczynski, *Phys Rev.*, **94** (1954) 61-64.
49. C. Reale, *Czech J. Phys. B*, **21** (1971) 662-672.
50. Z.H. Meiksin, *Thin Films*, **1** (1968) 211-221.
51. C.R. Pichard, C.R. Tellier and A.J. Tosser, *Phys. Stat. Sol. b*, **99** (1980) 353-358.
52. C.R. Tellier, C.R. Pichard and A.J. Tosser, *Electrocomp. Sci. 2 Technol.* **9,** (1981) 125-130.
53. C.R. Tellier and A.J. Tosser, *Thin Solid Films*, **52** (1978) 53-61.
54. F. Heintz and E. Zabler, *Sensors and Actuators*, **3** (1982/83) 327-341.
55. P. Thureau, *Symp.* Capteurs Français (Versailles, France, 1981), edited by La Documentation Française, Paris, 1982) p. 203-213.
56. C.A. Neugebauer in "Physics of thin films", vol. 2 - G. Hass and R.E. Thun, eds. (Academic Press, New York, 1964) p. 1-60.
57. R.W. Hoffman in "Physics of thin films", vol. 3 - G. Hass and R.E. Thun, eds .(Academic Press, New York, 1966) p. 211-273.
58. S.K. Sharma and O.P. Bahl, *Thin Solid Films*, **6** (1970) 239-248.
59. G.J. Van Gurp, *J. Appl. Phys.*, **46** (1975) 1922-1927.
60. A. Gangulee, *J. Appl. Phys.*, **43** (1972) 3943-3948.
61. C.R. Pichard, C.R. Tellier and A.J. Tosser, *J. Phys. D: Appl. Phys.*, **13** (1980) 1325-1329.

62. D.D. Thornburg and C.M. Wayman, *J. Appl. Phys.*, **40** (1969) 3007–3013.
63. D.E. Hill, L. Williams, G. Mah and W.L. Bradley, *Thin Solid Films*, **40** (1977) 263–270.
64. M. Laugier, *Thin Solid Films*, **67** (1980) 163–170.
65. K.L. Chopra, S.K. Bahl and M.R. Randlett, *J. Appl. Phys.*, **39** (1968) 1525–1528.
66. M. Portat, A. Bruere, J.C. Godefroy and F. Helias, *Symp.* Capteurs Français, 1981 (La Documentation Française, Paris, 1981) p. 96–115.
67. K. Barua and D.C. Barua, *Indian J. Pure & Appl. Phys.*, **14** 91976) 496–497.
68. H.Y. Yu and W.F. Leonard, *Thin Solid Films*, **20** (1974) 383–389.
69. W.F. Leonard and S.F. Lin, *Thin Solid Films*, **11** (1972) 273–281.
70. H. Sugawara, T. Nagano, K. Uozumi and A. Kinbara, *Thin Solid Films*, **14** (1972) 349–365.
71. H. Sugawara, T. Nagano and A. Kinbara, *Thin Solid Films*, **21** (1974) 33–42.
72. T.T. Sheng, R.B. Marcus, F. Alexander and W.A. Reed, *Thin Solid Films*, **14** (1972) 289–298.
73. C.R. Tellier and A.J. Tosser, *Electrocomp. Sci. & Technol.*, **3** (1976) 85–89.
74. R.E. Hummel and H.J. Geier, *Thin Solid Films*, **25** (1975) 335–342.
75. J.P. Chauvineau et C. Pariset, *Surface Sci.*, **36** (1973) 155.
76. C. Pariset et J.P. Chauvineau, *Surface Sci.*, **47** (1975) 543.
77. C.R. Pichard, C.R. Tellier and A.J. Tosser, *J. Mater Sci.*, **17** (1982) 10–16.
78. S.J. Raeburn and R.V. Aldridge, *J. Phys. F: Metal Phys.*, **8** (1978) 1917–1928.
79. R. Suri, A.P. Thakoor and K.L. Chopra, *Solid State Commun.*, **18** (1976) 605–608.
80. G. Wedler and W. Wiebauer, *Thin Solid Films*, **28** (1975) 65–81.
81. M. Inoue, Y. Tamaki and H. Yagi, *J. Appl. Phys.*, **45** (1974) 1562–1566.
82. S. Chaudhuri and A.K. Pal, *J. Appl. Phys.*, **48** (1977) 3455–3461.
83. C.R. Tellier, C.R. Pichard and A.J. Tosser, *Electrocomp. Sci. & Technol.*, **6** (1979) 19–22.
84. C.R. Pichard, C.R. Tellier and A.J. Tosser, *Electrocomp. Sci. & Technol.*, **7** (1981) 231–233.
85. A.F. Mayadas and M. Shatzkes, *Phys. Rev. B*, **1** (1970) 1382–1389.
86. G.R. Witt, *Thin Solid Films*, **13** (1972) 109–110.
87. P.M. Hall, *Appl. Phys. Lett.*, **12** (1968) 212.
88. B.S. Verma and H. Juretschke, *J. Appl. Phys.*, **41** (1970) 4732–4735.
89. J.C. Blair, C.R. Fuller, P.B. Ghate and C.T. Haywood, *J. Appl. Phys.*, **43** (1972) 307–311.
90. B. Bott, T.A. Jones and B. Mann, *Sensors and Actuators*, **5** (1984) 65–74.
91. A. Jones, T.A. Jones, B. Mann and J.G. Firth, *Sensors and Actuators*, **5** (1984) 75–88.
92. P.K. Clifford and D.T. Tuma, *Sensors and Actuators*, **3** (1983) 233–254.
93. P.K. Clifford and D.T. Tuma, *Sensors and Actuators*, **3** (1983) 255–282.
94. R. Lalauze and C. Pijolat, *Sensors and Actuators*, **5** (1984) 55–64.
95. J. Watson, *Sensors and Actuators*, **5** (1984) 29–42.
96. B. Bott and T.A. Jones, *Sensors and Actuators*, **5** (1984) 43–54.
97. P. Wissmann, *Thin Solid Films*, **13** (1972) 189–193.
98. J.P. Ganon, C. Nguyen Van Huong and J. Clavilier, *Surface Sci.*, **79** (1979) 245–248.
99. N.A. Surplice, J. Muller and B. Singh, *Thin Solid Films*, **28** 91975) 179–187.
100. G. Wedler and W. Wiebauer, *Thin Solid Films*, **28** (1975) 65–81.
101. A. Borodziuk-Kulpa, B. Stolecki and C. Wesolowska, *Thin Solid Films*, **67** (1980) 21–28.
102. G. Comsa, *Thin Solid Films*, **4** (1969) 1–14.
103. Z. Bastl, *Thin Solid Films*, **10** (1972) 311–313.